BARIC VARIATIONS OF THE OPTICAL PROPERTIES OF ROCHELLE SALT CRYSTALS

M.O. ROMANYUK, V.YO. STADNYK

UDC 535.323,535.53,537.226,548

Ivan Franko Lviv National University
(8, Kyrylo and Mefodii Str., Lviv 79005, Ukraine; e-mail: vasylstadnyk@ukr.net)

The influence of the uniaxial mechanical stress $\sigma_m \leq 200$ bar on the spectral (300—800 nm) and temperature (77—320 K) dependences of the refractive indices n_i ($i = x, y, z$) and the points of the birefringence sign inversion (BSI) of Rochelle salt (RS) crystals in the near infrared range has been studied. The parameters of the electron polarizabilities α_i and refractions R_i, as well as the parameters λ_{0i} and B_{1i} of UV oscillators of mechanically clamped RS crystals, have been calculated. The temperature-spectral-baric diagram of the BSI points of RS crystals has been plotted. The anomalies of the birefringences Δn_i in the vicinity of 200 K and the differences between the dependences $\Delta n_i(T)$ in nonpolar phases have been observed. These facts testify that the nonpolar phases are not identical, which is assumed to be caused by antipolarization. The baric changes of $n_i(\sigma)$ have been demonstrated to be due to the variation of the oscillator concentration (by about 30%), the shift of the absorption band edge, the effective band maximum, and the oscillator strength (by about 70%).

1. Introduction

The influence of the pressure p upon the dielectric and optical properties of Rochelle salt $KNaCaH_4O_6{\cdot}4H_2O$ crystals has been studied in a number of works (see, e.g., works [1–4]), and the attention to such researches is renewed [5–8].

Under the action of hydrostatic pressure, the initial dielectric permittivity has been demonstrated to vary, the upper Curie point to be shifted by 0.0107 K/atm, and the lower one by 0.0038 K/atm, so that the interval where the polar phase exists becomes narrower. If a specimen is subjected to uni- or biaxial squeezing conjugated to its spontaneous deformation, the dielectric hysteresis loops become asymmetric and distorted. At high pressures, they degenerate into a straight line with a slope close to that of the saturation section of the hysteresis loop of a free specimen. By analyzing the baric dependence of the temperature, at which the domains disappear, the Curie temperature of the specimens with the faces at 45° to their axes has been found to increase, if those specimens are subjected to the uniaxial squeezing, and to decrease in the case of the biaxial squeezing. The numerical values that were obtained for $\partial T/\partial p$ substantially differ from the data deduced from dielectric measurements [1], but agree with the data of work [8].

A lot of attention has been paid recently to the theoretical study of how the pressure influences the dielectric properties of ferroics, including RS crystals [5–9]. It has been shown that, while considering the Mitsui model, the account of terms connected to the shear deformation ε_4 improves the agreement between theoretical results and experimental data for spontaneous polarization and provides the correct temperature behavior of the relaxation times and the dynamic dielectric permittivity of RS in the vicinity of the phase transition (PT) point. The influence of various factors on the dielectric permittivity of RS crystals and the positions of their PT points have been studied in work [8].

In work [9], the influence of a uniaxial stress on the birefringence in RS crystals has been investigated, and the temperature and the spectral dependences of their absolute and combined piezooptic coefficients, as well as the BSI points, in the UV range of the spectrum have been found.

This work aims at studying the influence of uniaxial stresses on the spectral and temperature variations of the refractive indices of RS crystals and the shifts of their BSI points in the IR range of the spectrum.

2. Experimental technique

The baric variations of the refractive indices $n_i(\lambda, T)$ ($i = x, y, z$) were calculated, making use of the known temperature and spectral dependences of the absolute piezooptic coefficients π_{im} [9] and the refractive indices n_{io} of a mechanically free crystal [10], by the relationship

$$n_i(\lambda, T) = n_{io}(\lambda, T) - 1/2\pi_{im}(\lambda, T)\sigma_m n_{io}^3(\lambda, T). \qquad (1)$$

The birefringences Δn_i were calculated by analyzing the interference pattern created by polarized rays, the extrema k of which were determined by the difference

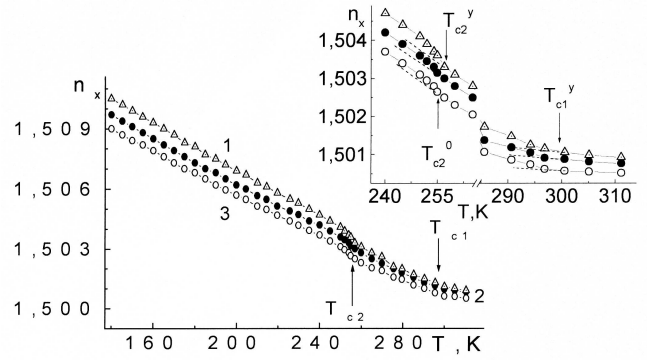

Fig. 1. Temperature dependences of the refractive index n_x of an RS crystal at $\lambda = 500$ nm: $\sigma_y = 200$ bar (*1*), $\sigma_z = 200$ bar (*2*), and $\sigma_i = 0$ (*3*). The temperature variations of n_x in the vicinity of the PT point are shown in the inset

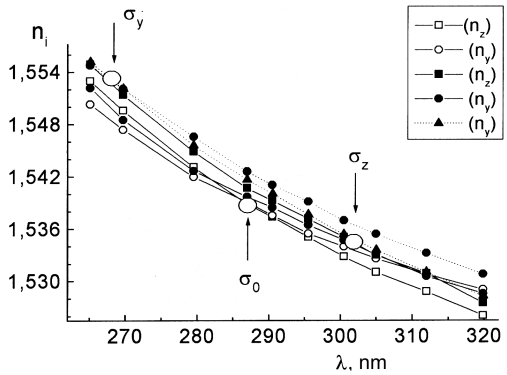

Fig. 2. Dispersion curves of the refractive indices of an RS crystal in the vicinity of the BSI point for various applied stresses: σ_z (solid) and σ_y (dotted curves). The measurements were done at room temperature. Hollow points correspond to the mechanically free crystal, and solid points to the mechanically clamped one

between the optical paths

$$\Delta n_i = d(n_j - n_m) = k\lambda, \tag{2}$$

with the temperature dependence of the crystal thickness d in the translucence direction being taken into account [11]. The positions of the PT points were found by considering the anomalies observed in the $\Delta n_i(T)$ dependences, and the BSI points by the conditions $\Delta n_i = 0$.

3. Results and Their Discussion

3.1. Influence of Uniaxial Stresses on the Refractive Indices of RS Crystals

The uniaxial mechanical stresses along various crystallophysical axes were found to be responsible for the changes of the refractive indices δn_i different by amplitude and sign; in particular, we determined that $\delta n_z(\sigma_y = 200 \text{ bar}) = 4.1 \times 10^{-5}$, $\delta n_z(\sigma_x = 200 \text{ bar}) = -3.9 \times 10^{-5}$, $\delta n_y(\sigma_z = 200 \text{ bar}) = 3.7 \times 10^{-5}$, and $\delta n_y(\sigma_x = 200 \text{ bar}) = -3.1 \times 10^{-5}$.

In Fig. 1, the temperature dependences of the parameter n_x, which were obtained provided that the RS crystal was subjected to the action of the σ_z or the σ_y stress of 200 bar, are shown. The temperature variations of n_i are nonlinear, with $dn_i/dT < 0$ and $|dn_y/dT| < |dn_x/dT| \approx |dn_z/dT|$ within the whole investigated spectral and temperature ranges. At the PT points, there are certain anomalies in the dependence $n_i(T)$, which are connected with the spontaneous electrooptical effect (EOE).

T a b l e 1. Spontaneous increments of the refractive indices δn_i of RS crystals in the vicinity of their PT point at $\lambda = 500$ nm and for various directions of the stress application ($\sigma_m = 200$ bar)

	σ_x		σ_y		σ_z	
T, K	250	290	250	290	250	290
δn_x			2.6	2.7	3.7	3.1
δn_y	3.4	3.1			4.2	4.0
δn_z	2.7	2.2	1.7	1.1		

The spontaneous increments δn_x of the refractive index n_x for a mechanically free RS crystal are somewhat smaller than those for a clamped one: $\delta n_x = 3.1 \times 10^{-4}$, 2.7×10^{-4}, and 2.4×10^{-4} at $T = 290$ K, and $\delta n_x = 3.7 \times 10^{-4}$, 2.6×10^{-4}, and 1.8×10^{-4} at $T = 250$ K for the stresses $\sigma_z = 200$ bar, $\sigma_y = 200$ bar and $\sigma_i = 0$, respectively.

The slopes of the linear sections of the curves $n_i(T)$ for the high- and low-temperature phases do not coincide. In particular, at $T < T_{c1}$, $dn_x/dT = 0.77 \times 10^{-5}$ for $\sigma_i = 0$ and 1.61×10^{-5} for $\sigma_y = 200$ bar, whereas, at $T < T_{c2}$, this quantity amounts to 6.25×10^{-5} for $\sigma_i = 0$ and 6.68×10^{-5} for $\sigma_y = 200$ bar; i.e. the slopes are steeper in the low-temperature phase, which can be explained by the spontaneous antipolarization and its baric dependence and testifies that those phases are not identical. The baric dependence of the spontaneous antipolarization can be calculated, making use of the knowing piezooptic coefficients and the measured values for Δn_i or n_i. The BSI point is the third characteristic temperature of RS crystals.

In Fig. 2, the fragments of the spectral dependences of n_i of an RS crystal in the vicinity of its BSI point ($\lambda_0 \approx 287$ nm) are depicted. The figure demonstrates that, as the specimen is subjected to the σ_y or σ_z stress,

the curves $n_i(\lambda)$ elevate, and the BSI point moves along the spectrum: at $\sigma_z = 200$ bar, $n_z = n_y = 1.53465$ and $\lambda_0 \approx 302$ nm; whereas at $\sigma_y = 200$ bar, $n_z = n_y = 1.55342$ and $\lambda_0 \approx 268$ nm. Below the BSI point, the dispersion of the dependence $n_i(\lambda)$ is smaller than that above λ_0. For clamped specimens, this difference becomes more pronounced.

Consider the correlation between the $n_i(\lambda, \sigma)$ dependences and other characteristics of the crystal, which follow from the Selmeier dispersion formula and the Lorenz-Lorentz formula, the latter describing the refraction R and the electron polarizability α:

$$n_i^2 = 1 + \frac{B_{1i}\lambda^2\lambda_{01}^2}{\lambda^2 - \lambda_{01}^2} + \frac{B_{2i}\lambda^2\lambda_{02}^2}{\lambda_{02}^2 - \lambda^2}, \tag{3}$$

$$\alpha = \frac{3}{4\pi N}\frac{n^2-1}{n^2+2}, \tag{4}$$

$$R = 4\pi/3N_A\alpha = \frac{\mu}{\rho}\frac{n^2-1}{n^2+2}. \tag{5}$$

Here, N is the number of particles per unit volume; N_A the Avogadro constant; μ the molar mass; ρ the density of the crystal; λ_{01} and λ_{02} are the wavelengths at the maxima of the absorption bands of UV and IR oscillators, respectively; $B_1 = \frac{e^2 f}{\pi m c_0^2}$ is the effective strength of an UV oscillator; e and m are the electron charge and mass, respectively; c_0 is the speed of light in vacuum; and f the oscillator strength.

Making use of the obtained dependences $n_i(\lambda, \sigma)$ and the formulas displayed above, we calculated the values of the parameters which are quoted in Table 2. One can see from the table that, at stresses of about 200 bar, the parameters α_i increase by about of 2×10^{-26} cm^3 on the average, which coincides, by the order of magnitude, with baric variations of the specimen's volume and its linear dimensions along the squeezing direction calculated on the basis of the Hooke law

$$(\Delta l/l_0)_i = s_{im}\sigma_m, \tag{6}$$

where $(\Delta l/l_0)_i$ are the relative stretchings, and s_{im} the components of the elastic compliance tensor. Provided that $\sigma_m \approx 200$ bar and $s_{im} \approx 10^{-11}$ m^2/N [12], we obtain that $(\Delta l/l_0)_i \approx 10^4$.

From Eq. (5), we obtain the relationship

$$\frac{dR}{d\sigma} = -\left(\frac{\mu}{\rho^2}\frac{n^2-1}{n^2+2}\frac{d\rho}{d\sigma}\right)_n + \left(\frac{\mu}{\rho}\frac{6n}{(n^2+2)^2}\frac{dn}{d\sigma}\right)_N \tag{7}$$

which allows the contributions of the components, which include the derivatives $\partial\rho/\partial\sigma$ and $\partial n/\partial\sigma$, to the baric variations of R_i to be evaluated. Using the numerical data $\mu = 282$ g/mol, $\rho \approx 1.56$ g/cm^3, $\partial\rho/\partial\sigma \approx s_{im} = 0.4\times10^{-10}$ bar^{-1}, $n_i = 1.5$, and $\partial n/\partial\sigma \approx 5\times10^{-6}$ bar^{-1}, we obtain 2×10^{-4} bar^{-1} for the first term in Eq. (7) and 4.8×10^{-4} bar^{-1} for the second, i.e. the contribution of the geometrical factor is about 30% of the total baric increment of R.

On the basis of the Selmeier formula for a single oscillator, we obtain

$$\frac{\partial n}{\partial\sigma} \approx \frac{1}{2n}\frac{e^2}{\pi m c_0^2}\left\{\frac{\lambda^2\lambda_0^2}{\lambda^2-\lambda_0^2}\left[f\frac{\partial N}{\partial\sigma} + N\frac{\partial f}{\partial\sigma}\right] + \right.$$

$$\left. + \frac{2Nf\lambda_0\lambda^4}{(\lambda^2-\lambda_0^2)^2}\frac{\partial\lambda_0}{\partial\sigma}\right\} = 0,03\frac{\partial f}{\partial\sigma} + 10^{-7}f + 3\cdot10^{-6}f\frac{\partial\lambda_0}{\partial\sigma}, \tag{8}$$

whence it follows that the dominating contributions to the baric variations of the refractive indices are given by the components that include the derivatives $\partial\rho/\partial\sigma$ and $\partial n/\partial\sigma$.

Knowing the baric variations of the refractive indices n_i enables the corresponding alterations of the energy gap width E_g to be estimated by Moss's relationship [13]

$$n^4 E_g = \text{const}, \tag{9}$$

whence it follows that

$$\frac{\partial E_g}{\partial\sigma} = -\frac{4}{n}E_g\frac{\partial n}{\partial\sigma}. \tag{10}$$

T a b l e 2. Baric dependences of the electron polarizability α_i, the specific refraction R_i at $\lambda = 500$ nm, and the parameters of effective oscillators in the Selmeier single-oscillator formula for an RS crystal at $T = 294$ K

Parameters	σ_i=0	σ_x=200 bar	σ_y=200 bar	σ_z=200 bar
$\alpha_x \times 10^{24}$, cm^3	18.370	18.395	18.396	18.394
$\alpha_y\times10^{24}$, cm^3	18.260	18.305	18.312	18.291
$\alpha_z\times10^{24}$, cm^3	18.190	18.407	18.412	18.394
R_x, cm^3	46.351	46.370	46.369	46.368
R_y, cm^3	46.081	46.113	46.097	46.092
R_z, cm^3	45.896	46.001	45.912	45.994
λ_{0x}, nm	109.67	109.38	108.95	109.92
λ_{0y}, nm	105.60	106.31	106.10	106.24
λ_{0z}, nm	108.99	108.28	109.89	108.56
$B_x\times10^6$, nm^{-2}	100.1	100.5	101.2	100.0
$B_y\times10^6$, nm^{-2}	108.8	107.8	110.1	111.1
$B_z\times10^6$, nm^{-2}	102.6	104.2	101.9	103.1

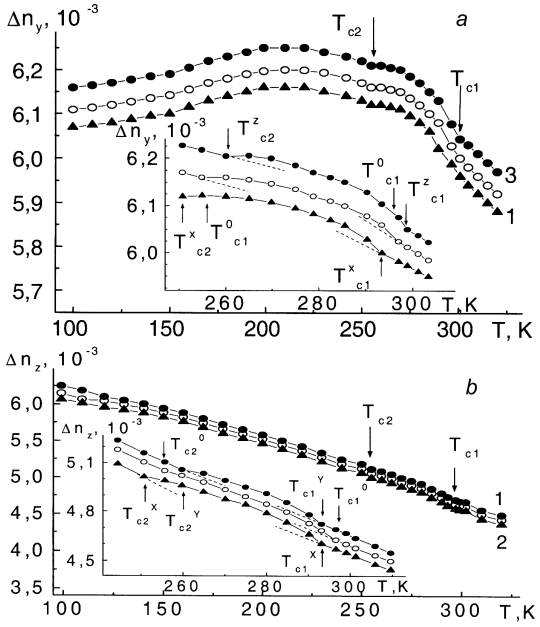

Fig. 3. Temperature variations of the birefringences Δn_y (*a*) and Δn_z (*b*) of the RS crystals at $\lambda = 500$ nm for various directions of a 200-bar stress: σ_x (*1*), σ_y (*2*), and σ_z (*3*). Hollow points correspond to the mechanically free specimen, and solid points to the mechanically clamped one. The variations Δn_y and Δn_z in the vicinity of the PT points T_{c1} and T_{c2} are shown in the insets

Taking the known values $\partial n/\partial\sigma \approx \times 10^{-6}$ bar^{-1}, $n_i \approx 1.5$, and $E_g \approx 5.1$ eV into account, we find $\partial E_g/\partial\sigma \approx 2 \times 10^{-5}$ eV/bar, which agrees with the results of the direct studies of the baric shift of the fundamental absorption edge of an RS crystal.

In order to determine the baric shift of the fundamental absorption edge of RS, we repeated the routine of measuring the absorption in the range of phonon manifestations [14], using the clamped specimens, and revealed the following. For a free RS crystal, $E_{gx} = 5.125$ eV, $E_{gy} = 5.152$ eV, and $E_{gz} = 5.162$ eV. At the same time, the energy gap width E_{gx} amounts to 5.121 eV if $\sigma_z = 200$ bar and to 5.119 eV if $\sigma_y = 200$ bar, i.e. $\partial E_g/\partial\sigma_z = 2 \times 10^{-5}$ eV/bar and $\partial E_g/\partial\sigma_y = 3 \times 10^{-5}$ eV/bar.

The baric shift of the effective UV oscillator – $\partial\lambda_0/\partial\sigma \approx (2 \div 4) \times 10^{-2}$ Å/bar $\approx 25 \times 10^{-5}$ eV/bar – turned out larger, which may be connected with its "location" in a higher-energy interval of the spectrum as compared to that of a real one (at about 7 eV). Therefore, its displacement has to be formally larger in order to achieve the agreement with experiment.

3.2. Influence of uniaxial stresses on the birefringences in and the BSI points of the RS crystals

In Fig. 3, the temperature variations of the birefringences Δn_y and Δn_z of RS crystals are plotted. As is seen from the figure, the variation Δn_y is characterized by a complicated behavior: as the temperature decreases, the dependence $\Delta n_y(T)$ grows, reaches the maximum at $T \approx 200$ K, and starts to fall down. In the case of the $\Delta n_z(T)$ dependences, such features are less pronounced. The temperature, at which the change of the sign of the temperature factor of birefringence $d\Delta n_y/dT$ ($d\Delta n_y/dT \approx -5.35 \times 10^{-7}$ K^{-1} at $T > 200$ K and $+8.85 \times 10^{-7}$ K^{-1} at $T < 200$ K) is observed, coincides with the temperature of abnormal variations of other parameters of the crystal [15–17], which evidences for the existence of the third critical temperature in RS crystals.

Some insignificant anomalies in Δn_y and Δn_z are also observed in the vicinity of the PT points, being more manifested at the lower-temperature PT. The slopes of the linear sections of the high-temperature ($d\Delta n_y/dT = -0.416 \times 10^{-6}$ K^{-1} and $d\Delta n_z/dT = -9.13 \times 10^{-6}$ K^{-1}) and low-temperature ($d\Delta n_y/dT = -7.71 \times 10^{-6}$ K^{-1} and $d\Delta n_z/dT = -0.301 \times 10^{-6}$ K^{-1}) paraphases are different, which may testify that those phases are not identical.

In their turn, the anomalies in the temperature behavior of the quantities Δn_y and Δn_z evidence for a certain "non-homogeneity" of the low-temperature RS phase.

The uniaxial stresses do not affect the dependences Δn_i qualitatively: the curves $\Delta n_y(T)$ become either elevated ($\sigma_z \neq 0$) or lowered ($\sigma_x \neq 0$); similarly, the curves $\Delta n_y(T)$ become shifted towards either greater ($\sigma_x \neq 0$) or smaller ($\sigma_y \neq 0$) birefringence values. The slopes of the curves for the high-temperature paraphase also vary: $d\Delta n_y/dT = -4.28 \times 10^{-7}$ and -4.02×10^{-7} K^{-1} for the stresses σ_z and σ_x, respectively; and $d\Delta n_z/dT = -9.25 \times 10^{-7}$ and -9.01×10^{-7} K^{-1} for the stresses σ_y and σ_x, respectively.

The uniaxial stresses displace the PT points considerably. In particular, the point T_{c1}, under the influence of the 200-bar stress σ_x or σ_z, becomes shifted towards a lower ($T_{c1} = 295.1$ K) or a higher ($T_{c1} = 299.3$ K) temperature, respectively. In this case, the corresponding baric coefficients of the PT point displacement amount to $\partial T_{c1}/\partial\sigma_x \approx -0.012$ K/bar and $\partial T_{c1}/\partial\sigma_z \approx +0.098$ K/bar.

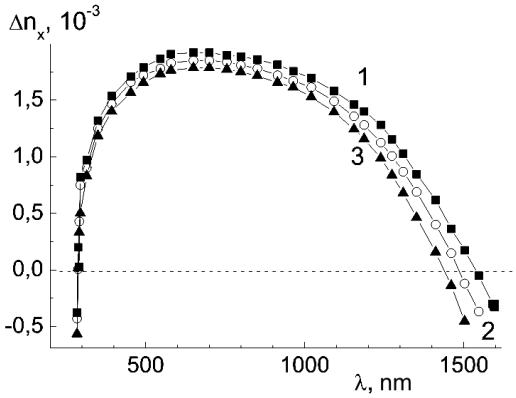

Fig. 4. Dispersion curves for the birefringence Δn_x of an RS crystal at room temperature for various directions of the uniaxial stress $\sigma_m = 150$ bar: σ_z (*1*), $\sigma = 0$ (*2*), and σ_y (*3*)

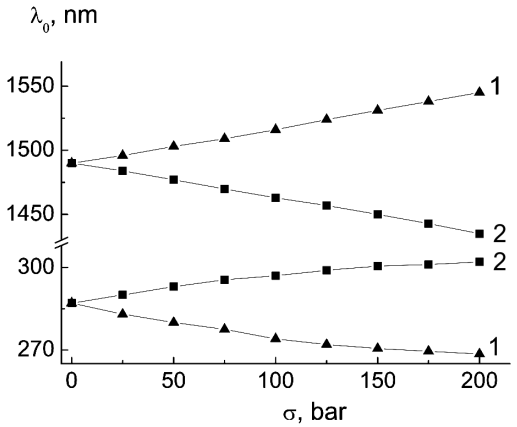

Fig. 5. Baric displacements of the BSI points of an RS crystal at $T = 294$ K: σ_z (*1*) and σ_y (*2*)

The BSI of RS crystals reveals itself along the X axis. In accordance to that, the spectral dependences of Δn_x in RS crystals subjected to the uniaxial σ_y or σ_z stress at room temperature are depicted in Fig. 4. The figure shows that, as the light wavelength grows, the amplitude of Δn_x increases drastically; at $\lambda \approx 500$ nm, the dispersion $d\Delta n_x/d\lambda$ decreases substantially; and, within the range $\lambda \approx 610 \div 690$ nm, Δn_x remains almost constant ($d\Delta n_x/d\lambda \approx 0$).

The further increase of the wavelength results in reducing Δn_x and growing its dispersion ($d\Delta n_x/d\lambda = 1.23 \times 10^{-6}$ nm^{-1}). The extrapolation of the curve obtained until it intersects the straight line $\Delta n_x = 0$ enabled us to determine the position of the second BSI point, namely, $\lambda_{02} \approx 1490$ nm at room temperature.

Since the stresses along Z and Y axes bring about the variations Δn_x, which are different by sign and amplitude, the spectral position of the BSI points is also changed. In Fig. 5, the baric displacements of the BSI points in the near UV [17] and IR ranges are shown. The figure demonstrates that the uniaxial stress σ_y shifts the UV BSI point towards the long-wave range at a rate $d\lambda_0/d\sigma_y = 0.0725$ nm/bar, and the IR BSI point towards short waves ($d\lambda_0/d\sigma_y = -0.095$ nm/bar).

Extrapolating the obtained dependences $\lambda_0 = f(\sigma_m)$ or solving the equation

$$\lambda_{01} + (d\lambda_{01}/d\sigma)\sigma_y = \lambda_{02} + (d\lambda_{02}/d\sigma)\sigma_y, \qquad (11)$$

provided that $d\lambda_{0i}/d\sigma$ are constant, one can establish that, if the stress $\sigma_y \approx 7.2$ kbar is applied, these BSI points "merge" together at $\lambda_{02} \approx 810$ nm. A similar situation occurs in $(NH_4)_2BeF_4$ crystals, but it is realized there through varying the temperature of the specimen [18].

The uniaxial stress σ_z moves, on the contrary, the BSI points apart: the first point makes its way towards the UV-range at a rate $d\lambda_{01}/d\sigma = -0.094$ nm/bar, and the second towards the IR-range at a rate $d\lambda_{02}/d\sigma = 0.185$ nm/bar.

The temperature variation also stimulates the shift of the BSI points. Therefore, we may draw a conclusion that the IR BSI point should shift towards the long-wave range of the spectrum if the temperature would rise, and towards the visible spectral range otherwise. The evaluation of the temperature-induced displacements of the BSI points of the RS crystal showed that, provided $T \approx 332$ K, they should coincide at $\lambda_0 \approx 737$ nm, and, in such a case, a "double" BSI point would emerge, as it does in FBA crystals [18]. However, RS crystals do not withstand the heating above 340 K and the uniaxial stresses of about 8 kbar; therefore, one may only talk about a hypothetical "double BSI point" in the RS crystal.

The corresponding temperature-spectral diagram for the UV BSI point of RS crystals is already known [17]. The temperature-induced displacement for the IR BSI point can be determined on the basis of the known temperature dependences of Δn_x. Taking advantage of the obtained baric dependences of the spectral position of the IR BSI point and the known diagram for the UV BSI one, we have plotted the temperature-spectral-baric diagram of the isotropic state of the RS crystal in the wide temperature (77—300 K), spectral (240–2300 nm), and baric (0–200 bar) ranges (see Fig. 6), which may be of use while applying this crystal as a crystallooptical sensor of temperature and pressure.

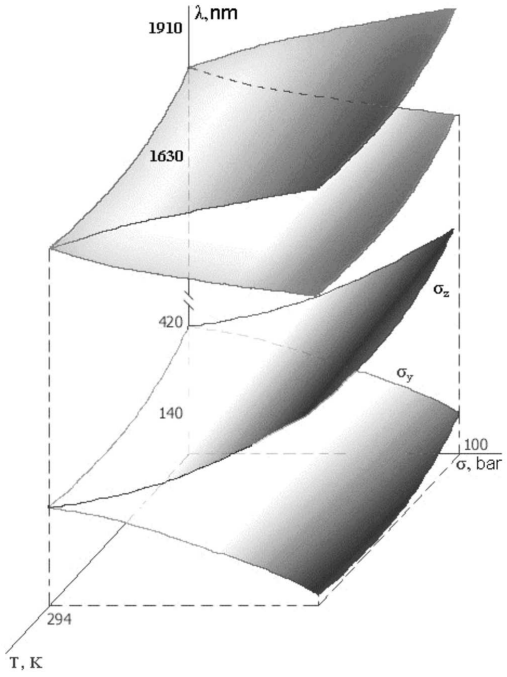

Fig. 6. Temperature-spectral-baric diagram of the isotropic state of the RS crystal

4. Conclusions

In this work, the baric variations of the refractive indices have been studied, the BSI point in the near IR-range has been investigated, and the electron polarizabilities α_i and refractions R_i, as well as the parameters λ_{0i} and B_{1i} of UV oscillators, of mechanically deformed RS crystals have been calculated. On the basis of the results obtained, it has been found that the uniaxial stresses increase the refractions R_i and the polarizabilities α_i and modify the parameters of effective oscillators.

It has been shown that the growth of the refractive index under the action of a uniaxial stress is mainly caused by the growth of the refractions (about 70% of the total effect), which takes place owing to the change of the energy gap width E_g ($dn/d\sigma \approx 10^{-6}$ bar^{-1} and $dE_g/d\sigma \approx 2 \times 10^{-5}$ eV/bar) and the long-wave shift of the UV absorption band maximum, and the concentration of effective oscillators (about 30% of the total effect) in the RS crystal.

The displacement of the IR BSI point under the influence of uniaxial stresses has been studied, which enabled us to describe a wide range of the spectrum by varying the amplitude and the direction of the specimen squeezing. The anomalies of Δn_i at $T \approx 200$ K have been revealed, and the nonidentity of non-polar RS phases, as well as the possibility of antiferroelectric ordering in the low-temperature phase, has been confirmed.

1. *Mason W.P.* Piezoelectric Crystals and Their Applications to Ultrasonics. — Princeton, New Jersey: D. Van Nostrand, 1950.
2. *Zheludev I.S., Romanyuk N.A.* // Kristallogr. — 1959. — **4**, N 5. — P. 710—717.
3. *Zheludev I.S., Romanyuk N.A.* // Ibid. — 1966. — **11**, N 4. — P. 610—613.
4. *Mori K., Hayashi M.* // J. Phys. Soc. Jap. — 1974. — **33**, N 5. — P. 1396—1400.
5. *Levitskii R.R., Zachek I.R., Verkholyak T.M., Moina A.P.* // Cond. Matter Phys. — 2003. — **6**, N 2(34). — P. 261—270.
6. *Levitskii R.R., Zachek I.R., Moina A.P., Andrusyk A.Ya.* // Ibid. — 2004. — **7**, N 1(37). — P. 111 — 139.
7. *Levitskii R.R., Zachek I.R., Verkholyak T.M., Moina A.P.* // Phys. Rev. B. — 2003. — **67**. — P. 174112-1 — 174112-12.
8. *Slivka A.G., Kedyulich V.M., Levitskii R.R. et al.* // Cond. Matter Phys. — 2005. — **8**, N 3. — P. 623—638.
9. *Stadnyk V.Yo., Romanyuk M.O., Vakhulovych V.F.* // Ukr. Fiz. Zh. — 1997. — **42**, N 10. — P. 1245—1251.
10. *Gaba V.M., Kostetskii A.M., Romanyuk N.A.* // Kristallogr. — 1989. — **34**, N 4. — P. 1041 — 1043.
11. *Romanyuk N.A., Kostetskii A.M.* // Fiz. Tverd. Tela. — 1976. — **18**.— P. 206—209.
12. *???*
13. *Moss T.S.* Optical Properties of Semiconductors. — New York: Academic Press, 1959.
14. *Romanyuk A.M., Viblyi I.F.* // Opt. Spektr. — 1976. — **41**, N 6. — P. 1011—1014.
15. *Gaba V.M., Romanyuk N.A., Franiv A.V.* // Ukr. Fiz. Zh. — 1982. — **27**, N 3. — P. 333—338.
16. *Poplavko Yu.M., Slesarenko N.V., Pasechnik L.A.* // Fiz. Tverd. Tela. — 1985. — **27**. — P. 1248.
17. *Dey P.K., Som K.K., Chowdhury K.R. et al.* // Phys. Rev. B. — 1993. — **47**, N 6. — P. 3001—3004.
18. *Romanyuk M.O., Stadnyk V.Y.* // Ferroelectrics. — 1997. — **192**, N 1—4. — P. 235—241.

Received 07.12.05.
Translated from Ukrainian by O.I. Voitenko

БАРИЧНІ ЗМІНИ ОПТИЧНИХ ВЛАСТИВОСТЕЙ КРИСТАЛІВ СЕГНЕТОВОЇ СОЛІ

М.О. Романюк, В.Й. Стадник

Р е з ю м е

Досліджено вплив одновісного механічного тиску $\sigma_m \leq 200$ бар на спектральну (300—800 нм) і температурну (77—320 К) залежності показників заломлення n_i і точку інверсії знака двопроменезаломлення (ІЗД) Δn_i кристалів сегнетової

солі в близькій інфрачервоній ділянці спектра. Розраховано електронні поляризовності α_i, рефракції R та параметри ультрафіолетових осциляторів (λ_{0i}, B_{1i}) механічно затиснутих кристалів. Побудовано температурно-спектрально-баричну діаграму ІЗД кристалів сегнетової солі. Виявлено аномалію Δn_i в околі 200 К та відмінності $\Delta n_i(T)$ у неполярних фазах, що свідчать про їх неідентичність та пов'язуються з наявністю антиполяризації. Показано, що баричні зміни $n_i(\sigma)$ зумовлені змінами концентрації осциляторів (на 30%), зміщенням краю поглинання і максимуму ефективної смуги та збільшенням сили осцилятора (на 70%).